Elastomers and Composites
Vol. 59, No. 4, pp. 137~148 (December 2024)
Print ISSN 2092-9676/Online ISSN 2288-7725
DOI: https://doi.org/10.7473/EC.2024.59.4.137

Prediction the Residual Life-time of Field-Aged FKM O-rings

Jin Hyok Lee[*], Myung Chan Choi[*], Yu Mi Yoon[*], Yongsu Jo[*], Yongwon Cho[*], Sung Han Park[**], Wonho Kim[***], Jong Woo Bae[*,†]

[*]*Elastic Material Research Group, Korea Institute of Materials Convergence Technology, Busan 47154, Republic of Korea*
[*]*Agency for Defense Development, Yuseong, Daejeon, 305-600, Republic of Korea*
[***]*Department of Chemical Engineering, Pusan National University, San 30 Jangjeon-dong, Geumjeong-gu, Busan 46241, Republic of Korea*

(Received November 11, 2024, Revised December 14, 2024, Accepted December 31, 2024)

Abstract: In this study, we analyzed the degradation behavior of fluoroelastomer (FKM) O-rings and established a correlation between the sealing force and equilibrium compression set, allowing us to predict the residual lifetime of field-aged FKM O-rings to be 12.3 years. An intermittent compressive stress relaxation (CSR) jig was designed based on the working mechanism of O-rings, enabling us to measure the sealing force of an FKM O-ring through intermittent CSR testing. The measured sealing force was 1.27 kN at room temperature. We observed the degradation behavior of FKM O-rings at various thermal aging temperatures and applied the time-temperature superposition (TTS) principle to obtain the stress relaxation master curve at 60°C. By analyzing the relationship between α_T and 1/temperature, we extrapolated α_T to be 0.088 at room temperature. We then constructed the stress relaxation master curve at room temperature and defined the failure condition as $F_t/F_0 = 0.2$, which led to a predicted lifetime for the O-ring of 66.2 years at room temperature. The compression set of the O-rings decreased over time at room temperature due to physical relaxation, which induced a recovery of O-ring thickness. We found that thermal treatment could accelerate this physical relaxation, allowing the O-rings to reach an equilibrium state in a shorter time. We recommend a thermal treatment condition of two days at 80°C. To assess the effects of chain scission and chain recombination, we measured stress relaxation in both strained and unstrained states. The average value of parameter a, representing the ratio of chain recombination to chain scission, was found to be 1.47, with a deviation of ±0.05. Because this value was greater than one, we confirmed that chain recombination was relatively dominant in the FKM O-rings throughout the aging process. Using empirical data on the sealing force and equilibrium compression set, we established a correlation between F_t/F_0 and the equilibrium compression set. To predict the residual lifetime, we examined 10 FKM O-rings that had been field-aged for 12.3 years in a propulsion unit. Following the recommended procedures, we measured the equilibrium compression set of these field-aged FKM O-rings to be 13.45%, with a deviation of ±4.6%. By analyzing the relationship between Ft/F0 and the equilibrium compression set, we calculated the value of Ft/F0 for the field-aged FKM O-rings to be 0.909. Utilizing the stress relaxation master curve at 23°C, we predicted the residual lifetime of the field-aged O-ring to be 56.3 years.

Keywords: FKM O-ring, intermittent compression stress relaxation (CSR), time temperature super-position (TTS), degradation behavior, equilibrium compression set, residual life-time

Introduction

Compared with metals or plastics, elastomers have unique characteristics: elastic and large deformation, so they are used in many kinds of industrial components Especially, O-rings are especially used in various industrial fields: pipes, autoclaves, plants, propulsion devices, missiles, aerospace, etc., for sealing fluids. In case of pipes, O-rings could be easily changed to new one. However, in case of plants, propulsion devices, and missiles, O-ring maintenance needs much time and cost. If O-ring maintenance is not suitable, it could induce the catastrophe.[1] For efficient O-ring maintenance, followings should be studied; 1) degradation behavior, 2) predicting the life-time, and 3) predicting residual life-time of O-ring.

For accurate analyzing the degradation behavior and predicting the life-time, one of the most important points was an accurate mimic of the environment of its application. In the past, compression set and tensile strength were usually used for analyzing the degradation behavior of O-rings. But

[†]Corresponding author E-mail: jwbae@kimco.re.kr

those were showed different results with actual O-rings. Also, recent studies largely use a diminutive sample of a small disc or washer; discs of diameter lower than 30 mm and washers of outer diameter lower than 42 mm. The use of a reduced sized sample could have the following problems: 1) the difference of size could lead to different stress responses to compression; 2) the different exposure area-to-total surface area ratio to atmosphere could lead to a different degradation rate; 3) data could be rendered unreliable as a diminutive specimen may have a different degree of crosslinking from an actual O-ring. In this study, we used actual O-rings; cross-sectional diameter is 3.53 mm, and inner diameter is 91.67 mm, for analyzing the degradation behavior and prediction the life-time. We measured sealing force of actual O-rings, not compression set or tensile strength.

Compression stress relaxation (CSR) testing is a typical method for measuring the sealing force of an O-ring and widely used for life-time prediction. CSR testing was standardized as an international standard, ISO 3384 in 1979. R. P. Brown and F. N. B. Bennett reported CSR test methods and evaluated its basic characteristics by the type of test jig.[2] CSR testing is divided into continuous CSR testing and intermittent CSR testing. The continuous CSR test is simple and commonly used. It observes a continuous change of sealing force. However, it requires expensive apparatus and is limited by the size and shape of the test jig. Intermittent CSR testing - also called “discontinuous CSR test” because the sealing force is measured periodically - is a suitable test method to mimic the circumstances of an O-ring’s application because there is no limitation in the size and shape of test jig and specimen. Intermittent CSR testing requires only simple and cheap apparatus such as a jig, an oven, and an universal testing machine (UTM). Tuckner reported the advantages and limitations of different CSR testers and jigs used for intermittent CSR testing, and also discussed the data of several intermittent CSR test cases.[3-5] S. Ronan *et al.* predicted the life-time of natural rubber by using both continuous and intermittent CSR tests.[6] We also reported predicting the life-time of chloroprene rubber O-ring and FKM O-ring by intermittent CSR method in the previous study.[7]

For some time, predicting the life-time of elastomers has been an important and interesting issue. The Arrhenius relationship is generally the method of first choice for doing this. It is based on the assumption that the rate of the degradation (k(T)) is proportional to exp(-E_a/RT). As shown in equation (1), a plot of ln k(T) against 1/T shows a linear relationship with a slope of E_a/R. By extrapolating to ambient temperature, life-time can be predicted.

$$k(T) = A\exp(\frac{-E_a}{RT}) \Leftrightarrow \ln k(T) = -\frac{E_a}{RT} + C \quad (1)$$

Where k(T) is the reaction rate for the process, E_a is the activation energy, R is the gas constant (8.314 J/mol K), T is the absolute temperature, and A is the pre-exponential factor(constant).

However, it is difficult to measure the reaction rate k(T), so frequently the time taken to reach a given % of the initial value of the physical properties is chosen instead of the reaction rate.

The method of predicting life-time using this relationship was standardized as international standard ISO11346. It has, however, been found that this method can give predictions of life-time that are too long. This arises from the assumption in the Arrhenius approach that the reaction rate at service temperature is same as that at test temperature, i.e. that activation energy is independent of temperature. However, activation energy has been found to vary with temperature.[8-11] Elastomers’ degradation and predictions of their life-times have been studied with a variety of techniques. In a review by Celina *et al*. the many techniques used to analyze elastomer degradation include modulus profiling, oxygen permeability, NMR, TGA and DTA.[12] By analyzing modulus profiling, oxygen permeability, and oxygen consumption rate, Gillen et al. monitored the change of activation energy with temperature and hence predicted elastomers’ life-times.[13-15] Eventually, it was found that activation energy decreased with decreasing degradation temperature, meaning that a life-time predicted at ambient temperature will be shorten than that observed at these high test temperatures. It was also found that elastomers show non-linear degradation behavior, something not taken into account by the Arrhenius approach.

In this study, we predicted the residual life-time of field-aged FKM O-rings, which had 91.67 mm inner diameter and 3.53 mm cross-sectional diameter. We observed degradation behavior of FKM O-rings by intermittent CSR testing. An intermittent CSR jig was designed by considering the application circumstances of an O-ring. By using time-temperature superposition (TTS) principle, we observed the degradation behavior of FKM O-rings at room temperature. We correlated relationship between sealing force and compression set. We standardized the method that predicting

the residual life-time of FKM O-rings. Also, we predicted residual life-time of 12.3 years field aged FKM O-rings.

Experimental Methods

1. Materials

Field-aged FKM O-rings which was jointed a propulsion unit during 12 years, were used. It was assembled by applying 25% compression ratio and silicon oil was used as a lubricant. The dimensions are 91.67 mm inner diameter and 3.53 mm cross-sectional diameter. For predicting the residual life-time we manufactured FKM O-rings which have same formulation and size with the field-aged FKM O-ring. FKM O-rings which have for testing were supplied from Sam Jung Industrial Co. (South Korea). Viton FC2181 (3M, USA) was used as main matrix of FKM O-rings. Chemical structure of FKM elastomer is poly(vinylidene fluoride)-co-hexafluoropropylene, and showed in Scheme 1. Table 1 showed the formulation of FKM O-rings. Silicon oil, SLUBE 884 (Parker, USA), was used as a lubricant for assembling.

2. Measurements

A convection oven, AS-F0-05 model of A-Sung Tester Co. (Korea), was used for the thermal aging tests. The temperature deviation was ±1°C between gauge and actual temperature.

An Instron (U.S.A) UTM, 3345(Q3776) model, was used

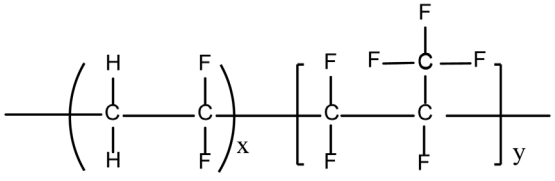

Scheme 1. Chemical structure of FKM elastomer.

Table 1. The Formulation of FKM O-ring.

Ingredients	FKM O-ring (phr)
Viton FC2181	100.0
Carbon black (N550)	46.0
Zinc oxide	3.0
Peroxide	3.0
Homogenizer	2.0
Stearic acid	1.0
Triallylisocyanurate	4.0

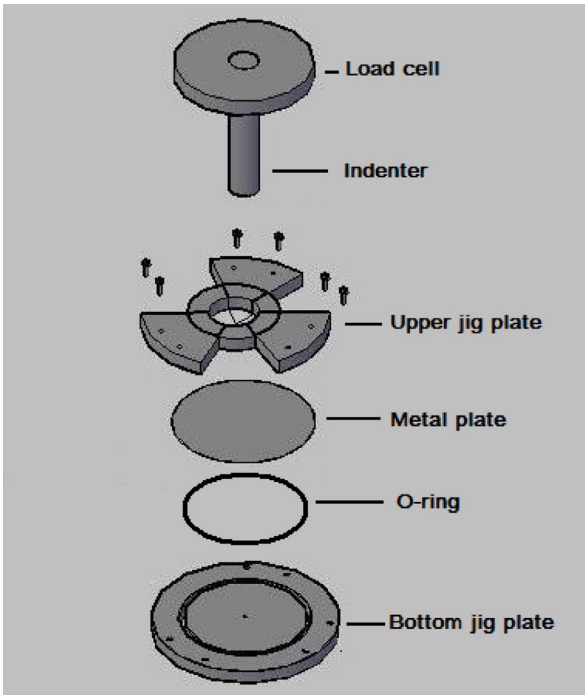

Figure 1. A jig for intermittent CSR test.

to measure the sealing force and 25% compressive modulus of the O-rings. The indenter was was cylindrical of dimensions 25 mm × 180 mm for measuring the sealing force and 120 mm × 25 mm (diameter × height) for measuring the 25% compressive modulus. The test speed was 1.0 mm/min. Data acquisition rate was 100 point/sec.

To perform the intermittent CSR test, the test jig was designed (Figure 1) and manufactured by the consideration of O-ring assembly. Stainless steel was selected for its construction to prevent corrosion. The diameter and thickness of the bottom jig plate were 180 mm and 30 mm, respectively. A circular groove on the bottom jig plate was designed according to KS B 2799 (O-ring housing design criteria; Korea Standard), and 0.1 mm free depth was guaranteed for further compression to determine the sealing force. The inner diameter, width, and depth of the groove were 92.79 mm, 4.75 mm, and 2.55 mm, respectively. The degree of parallelization of the bottom surface of groove relative to the surface of bottom jig plate was tested by a dial gauge. The dial gauge showed a deviation of only 0.01 mm, confirmed its suitability for intermittent CSR testing. Considering the O-rings; size (inner diameter is 91.67 mm), the metal plate which was to be pressed down by the indenter onto the O-ring was chosen to be 110 mm in diameter. Because of the 4.4 : 1 size ratio between the metal plate and diameter of indenter, a reduction of accuracy

of sealing force measurement by bending of the metal plate may have been a problem. However, the thickness of the metal plate (5.0 mm) was made sufficient to prevent this. The diameter and thickness of the upper jig plate were 180 mm and 30 mm, respectively. As shown in Figure 1, parts of the upper jig plate were removed to find out the centering of the metal plate. Some part of the upper jig plate acted as a shim of height 5.00 mm. After the jig was assembled, an O-ring was compressed to 2.65 mm: a compression ratio of 25%, the commercial guideline. The diameter of the central hole of the upper jig plate was chosen to be 30.0 mm by considering the diameter of the indenter. This design of the hole allowed the indenter to be set on the center of metal plate during intermittent CSR testing. The manufactured jig was 180 mm in diameter and 60 mm in height.

Intermittent CSR tests followed this procedure: 1) an O-ring was fitted to the jig; 2) the assembled jig was placed in a pre-heated convection oven; 3) the jig was periodically removed from the convection oven to measure the sealing force of the O-ring by using a UTM; and 4) after measurement, the jig was returned to the oven for continuous thermal aging testing.

A jig for compression set test were also designed and manufactured with consideration of how O-rings see service. A circular groove on the bottom jig plate was designed according to KS B 2799 (O-ring housing design criteria; Korea Standard). The inner diameter, width, and depth of the groove were 92.79 mm, 4.75 mm, and 2.65 mm, respectively. Other feature of a jig was same as a jig for intermittent CSR test. After the jig was assembled, an O-ring was compressed to 2.65 mm: a compression ratio of 25%. The manufactured jig was 180 mm in diameter and 60 mm in height.

Compression set could be easily determined by measuring the thickness of O-rings. Video-scope, model PWIDS-2M (PulsWin, Korea), was used to measure the thickness of the O-rings. For measuring the thickness, got a photograph enlarged with 60 times, and analyzed the thickness of O-ring with image analyzing program, ITPlus 5.0. Photo 1 showed video-scope apparatus and thickness measuring image. With measured thickness value, compression set was calculated by using equation (2).

$$\text{Compression set(CS)} = \frac{t_0 - t_t}{t_0 - t_c} \times 100 \quad (2)$$

Where, CS is the compression set (%), t_o is initial thickness of an O-ring (mm), t_f is final thickness of an O-ring, after removed from the compression set jig (mm), and t_c is thickness of an O-ring at compressed stated (mm).

Results and Discussion

1. Degradation behavior

1.1 Sealing force

Figure 2(a) showed results of an intermittent CSR test to measure the sealing force of a FKM O-ring at room temperature. Region 1 showed the indenter chamber and loaded into plate. Region 2 began the indenter making contact with the metal plate; its slope showed the stiffness of the component configuration (Line (a); 103.0 kN/mm). Region 3 had a slope indicative of the stiffness of the O-ring (Line (b); 13.3 kN/mm). The stiffness of the metal plate and a FKM O-ring showed different slopes. The intersection between Lines (a) and (b) was the sealing force of a FKM

(a) (b)

Photo 1. (a) Video-scope apparatus and (b) thickness measuring image.

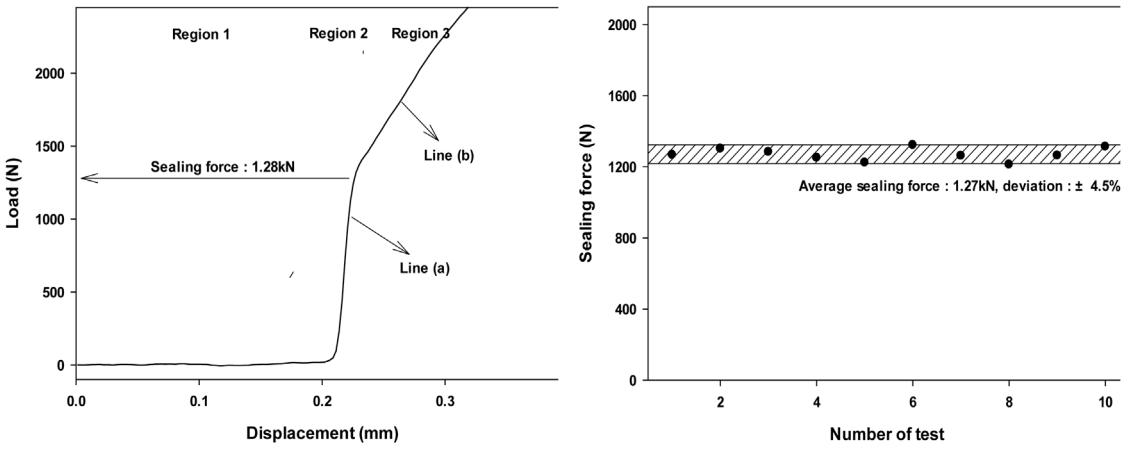

Figure 2. Sealing force of a FKM O-ring at 23°C; (a) load vs. displacement behavior of a FKM O-ring from intermittent CSR, and (b) sealing force according to the number of tests.

O-ring; from Figure 2 it was found to be 1.28 kN at room temperature.

Figure 2(b) showed sealing force of FKM O-rings according to the number of intermittent CSR test. Intermittent CSR test was repeated ten times at room temperature. Each intermittent CSR test used new O-rings. Average sealing force of O-ring was 1.27 kN, and deviation was ±4.5%. We confirmed that designed intermittent CSR jig and intermittent CSR test were suitable to measure the sealing force, in here.

1.2 Degradation behavior

Figure 3(a) showed results of compression stress relaxation of O-rings tested at 60°C, 80°C, 100°C, 120°C, and 170°C. F_t is the sealing force at time t, and F_0 is the initial sealing forces. With increasing aging time, residual sealing force was decreased and the degree of degradation was increased. With elevating aging temperature, degradation rate was increased. At 60°C and 80°C, degradation rate was too slow and sufficient degradation was not obtained. Even after over 5,208 hrs (217 days), F_t/F_0 was just 0.914 at 60°C. For observing degradation behavior at 60°C, the TTS principle was applied to the stress relaxation data. The results were shown in Figure 3(b). Shift factor, α_T, was calculated from the superposed empirical data. The time which a FKM O-ring took to reach 0.2 F_t/F_0, was respectively 48,760 hrs. Comparing with Figure 3(a), we could save about 43,552 hrs of testing time by using TTS principle. Figure 4 showed change of ln α_T according to 1000/T. In both cases,

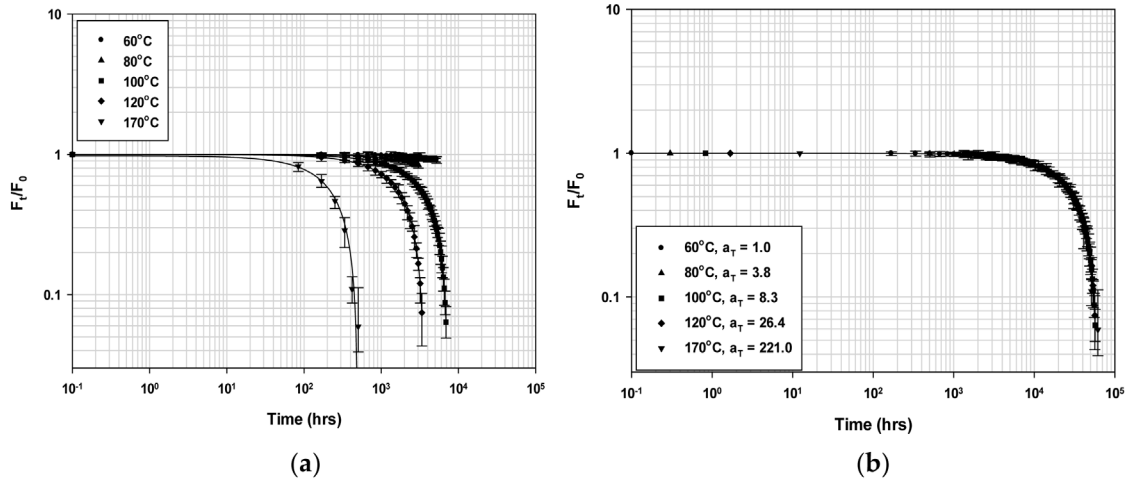

Figure 3. Stress relaxation of a FKM O-ring; (a) according to various aging temperature, and (b) master curve at 60°C.

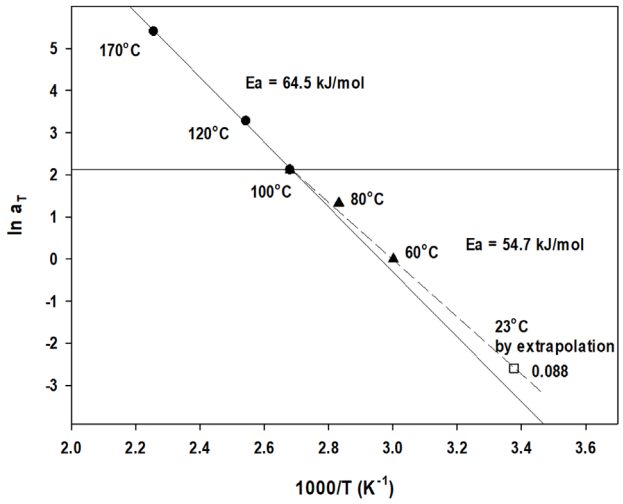

Figure 4. Arrhenius plot of shift factor, α_T.

i.e., at the case of high temperature (over 100°C) and low temperature (below 100°C), the Arrhenius relationship was shown between ln α_T and 1000/T. The activation energy was calculated by followed equation (3).

$$E_a = \frac{R ln \frac{a_{T2}}{a_{T1}}}{\frac{1}{T_2} - \frac{1}{T_1}} \quad (3)$$

At 100°C~170°C region, the activation energy was 64.5 kJ/mol. At 60°C~100°C region, the activation energy was 54.7 kJ/mol, lower than the activation energy of 100°C~170°C region. We reported that the activation energy being decreased at lower temperatures in previous study.[6] Shift factor, α_T, at room temperature (23°C) was calculated as 0.088 by extrapolation. Using the values of α_T (reference temperature is 23°C), we recalculated shift factor and could obtain the degradation master curve at 23°C as shown in Figure 5. Failure condition was selected as F_t/F_0=-.2, and shown as a dashed line. From Figure 5, life-time of a FKM O-ring predicted to be 66.2 years at room temperature.

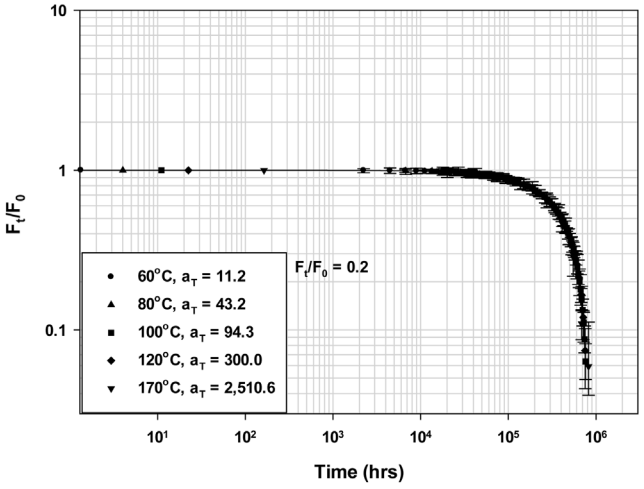

Figure 5. Stress relaxation master curve of a FKM O-ring at 23°C.

2. Equilibrium compression set

2.1 Recovery the physical relaxation

In fields, O-rings were installed to groove and compressed to pre-determined ratio to seal fluids. After installing, O-rings slowly degraded, and it induced decreasing the sealing force. Decreasing the sealing force was composed with physical relaxation and chemical relaxation. Physical relaxation was caused by the movement of chain towards new configuration in equilibrium at compressed condition, and was reversible. On the other hand, chemical relaxation was caused by scission and recombination events resulting from the breakage and formation of covalent bonds, and was irreversible.[16] So, when O-rings were removed grom groove and put the uncompressed condition, thickness of O-rings was slowly recovered with time. We observed the recovery of the physical relaxation with followed test; 1) O-rings were assembled to compression set jig and aged during 43 days at 120°C, 2) after aging process, O-rings were removed from jig and cooled at atmosphere, and 3) compression set of O-rings were measured with a video-scope during several months. Five FKM O-rings were used in this test. Figure 6(a) showed the change of compression set with time at room temperature. Because of physical relaxation induced recovery of O-ring thickness, compression set of O-rings was decreased with time at room temperature. After 420 days (14 months), change of the compression set was 15.7% and compression set was still decreasing. This phenomenon was caused by the recovery of physical relaxation, and compression set would be decreased until it arrived to equilibrium state.

2.2. Equilibrium compression set measurements

Caused by slow physical recovery, there needs long time to arrive new equilibrium state. For accuracy measurement of compression set, an acceleration process of physical relaxation is needed. K. T. Gillen and coworkers reported that thermal treatment could accelerate the physical relaxation and could be arrived new equilibrium state in a short time. We observed thermal treatment effect on the accelerating

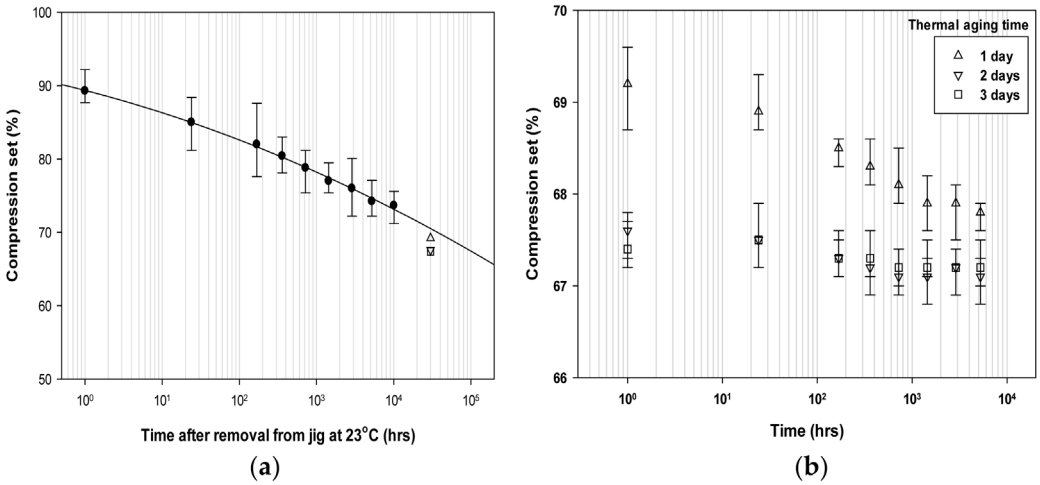

Figure 6. Change of compression set for FKM O-rings with time after removal from jigs; (a) non-treated, and (b) after thermal aging treatment.

physical relaxation with followed test; 1) O-rings were assembled to compression set jig and aged during 43 day at 120°C; 2) after aging process, O-rings were removed from jig and cooled at atmosphere, 3) O-rings aged with scheduled thermal treatment conditions; one day, two days, and three days at 80°C, 4) after thermal treatment, O-rings were cooled at atmosphere, and 5) compression set of O-rings were measured with video-scope during several months. Unfilled symbols of Figure 6(a) showed the change of compression set with time after thermal treatment. Unfilled triangle-up symbol which treated one day at 80°C showed 69.2% of compression set. This value was 20.1% lower than that of non-treated O-ring's compression set, and it estimated to compression set of non-treatment O-ring which kept during 2,039 days (5.6 years) at room temperature. We confirmed that thermal treatment greatly could accelerate physical relaxation. Unfilled triangle-down symbol and unfilled square symbol which each thermal treatment condition was 2 days and 3 days at 80°C, showed 67.7% and 67.4% of compression set. Theses values were 21.7% and 21.9% lower than that of non-treated one, and estimated to 4,384 days (12.0 years) and 4,551 days (12.5 years). With increasing time for thermal treatment, acceleration rate of physical relaxation would be increased. However, over 2 days thermal treatment, slowdown of acceleration rate was observed. Figure 6(b) showed the change of compression set of thermally treated O-ring with time at room temperature. During 218 days (7 months), unfilled triangle-up symbol which was thermally treated one day, showed 1.4% change of compression set. By one day thermal treatment, physical relaxation was accelerated, but it would not arrive to equilibrium state. On the other hand, unfilled triangle-down and unfilled square symbol which were thermally treated two and three days, showed 0.5% and 0.2% change of compression set with time. Over two days of thermal treatment, physical relaxation would be accelerated and arrived to new equilibrium state with short time. Three days of thermal treatment, showed lower compression set than two days of thermal treatment. However, difference of compression set between two days and three days of thermal treatment was under 0.3%. it could be supposed as data deviation. Therefore, two days of thermal treatment recommended for accelerating physical relaxation, and arriving to equilibrium state with short time. We set up the equilibrium compression set measurement procedure as follows; 1) FKM O-rings were emitted from jig at scheduled aging time, 2) FKM O-rings were cooled at room temperature during two hours, 3) FKM O-rings were thermally treated during two days at 80°C convection oven, 4) FKM O-rings were cooled at room temperature during two hours, and 5) thickness of O-ring was measured by video-scope and calculated equilibrium compression set.

3. Correlation between sealing force and equilibrium compression set

3.1. Chain scission and chain recombination effect on the degradation

In the degradation process, there were two main chemical reaction; chain scission and chain recombination. Chain scission occurred as breaking the molecular network by

oxidation and tended to be soften. On the other hand, chain recombination introduced new molecular network and tended to be harden. Tobolsky and coworkers reported that could observe both chain scission and chain recombination by stress relaxation at unstrained state, and could isolate chain scission effect by stress relaxation at strained state.[14] We already observed stress relaxation at strained state (See Figure 3(a)). Stress relaxation at unstrained state, was observed by measuring 25% compressive modulus of O-rings. Initial 25% compressive modulus is M_0, and 25% compressive modulus at time t is M_t. Figure 7 showed results of stress relaxation of FKM O-rings both strained and unstrained state at 120°C. Stress relaxation at strained state, F_t/F_0 was decreased by chain scission of molecular network. On the other hand, stress relaxation at unstrained state, M_t/M_0 was increased by forming new molecular network.

Tobolsky and coworkers suggested followed theoretical modeling expression and confirmed that the theoretical model was experimentally suitable to several rubbers.[16]

$$\% \text{ Permanent Set} = \frac{100\lambda\left[\frac{Q+\frac{F}{\lambda}}{Q+F\lambda^2}\right]^{1/3}}{\lambda-1} \quad (4)$$

Where, λ is the stretch ratio, F is F_t/F_0.

In their research, K. T. Gillen and coworkers defined parameter *a* for predicting the relative importance of chain scission and chain recombination.[17-18]

$$a = \frac{Q}{1-F} \quad (5)$$

F_t/F_0 is residual stress at strained state. Stress decay is induced by chain scission. So, 1-F means the quantity of chain scission. Also, Q means the quantity of chain recombination. Q also could be calculated as $M_t/M_0 - F_t/F_0$. When *a* is greater than unity, chain recombination is relatively dominate the chain scission, and tended to be harden. When *a* is unity, there was balance between chain scission and chain recombination. When *a* is less than unity, chain scission was relatively dominate chain recombination, and tended to be soften. From Figure 7, we calculated parameter *a* with empirical data, and shown in Table 2.

Average value of parameter *a* was 1.47, deviation was ±0.05. Parameter *a* showed uniform value distribution at whole aging processes. Because of it was greater than unity, we could confirm that chain recombination was relatively dominate chemical reaction of FKM O-rings at whole aging

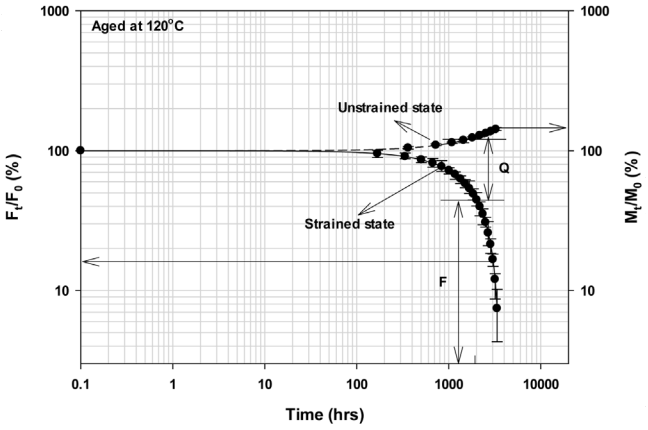

Figure 7. Stress relaxation with time-dependence both strained and unstrained state.

Table 2. Sealing (F_t/F_0), Chain Recombination (Q), and Parameter *a* of FKM O-rings at 120°C Aging Process.

F_t/F_0	Q	a
1.0	0.0	-
0.9	0.147	1.47
0.8	0.298	1.49
0.7	0.438	1.46
0.6	0.584	1.46
0.5	0.76	1.52
0.4	0.888	1.48
0.3	1.043	1.49
0.2	1.176	1.47
0.1	1.287	1.43
	Average	1.47
	Deviation	±0.05

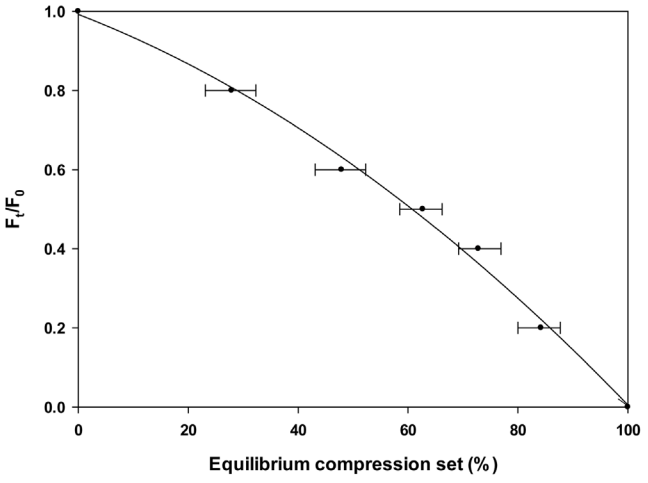

Figure 8. Relationship between F_t/F_0 and equilibrium compression set for FKM O-rings.

FKM O-rings, equilibrium compression set was measured as recommended procedure. Figure 8 showed correlation between sealing force and equilibrium compression set. We confirmed that there was non-linear relationship between sealing force and equilibrium set. Caused by this relationship, it was suitable to use sealing force for analyzing degradation behavior or predicting the life-time, instead of compression set or elongation. The stretch ratio was 0.75, and parameter *a* was 1.47 (defined from Eq. (3)). Because of parameter a was greater than unity, the curve showed convex shape. We could experimentally correlate between sealing force and equilibrium compression set.

3.4. Prediction of the residual life-time of field-aged FKM O-rings

For predicting the residual life-time, we took out ten FKM O-rings which were 12.3 years field-aged in a propulsion unit. We measured equilibrium compression set of field-aged FKM O-rings according to the equilibrium compression set measurement procedures. Equilibrium compression set of field-aged O-rings was 13.4%, and deviation was ±4.6%. By using the relationship between F_t/F_0 and equilibrium compression set, we could determine F_t/F_0 of field-aged FKM O-rings; as shown in Figure 9. F_t/F_0 of field-aged FKM O-rings was determined to 0.909. By using stress relaxation master curve at 23°C, we could predict the residual life-time of field-aged FKM O-rings. The result is shown in Figure 10. In previous section, the analyzed life-time of O-ring was 66.2 years at failure condition; $F_t/F_0 = 0.2$ (Region 1 + Region 2). At F_t/F_0 was 0.909, aged time was 9.9 years in

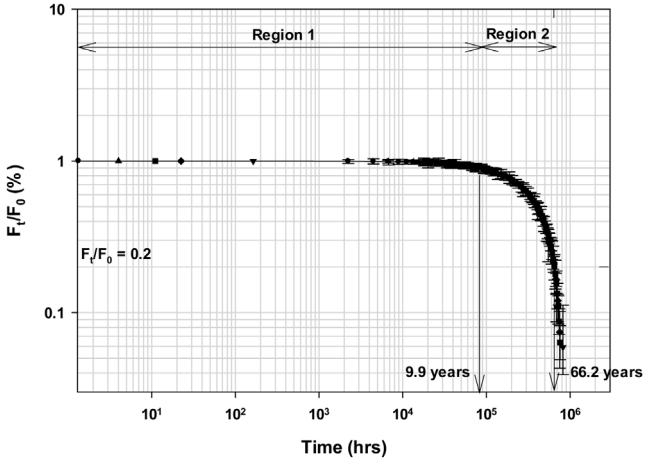

Figure 9. The conversion of equilibrium compression set to F_t/F_0 for 12.3 years field-aged FKM O-rings.

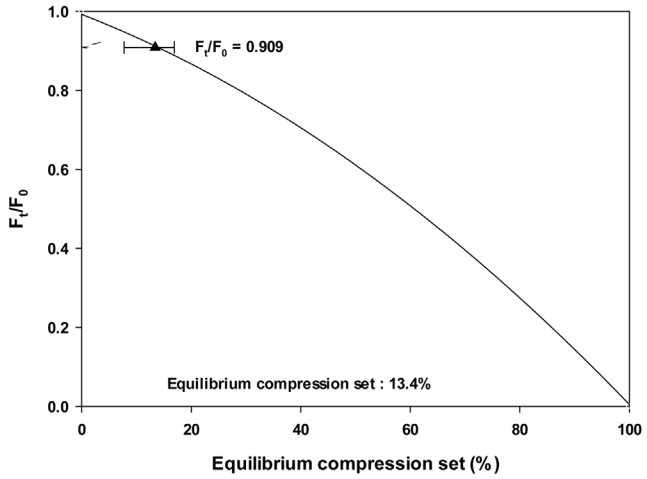

Figure 10. Prediction of the residual life-time for 12.3 years field-aged FKM O-rings.

Figure 10. It was shorter than field-aged time, 12.4 years. Considering the deviation of equilibrium compression set, the difference of aged time was small, and reasonably could be accepted. Therefore, Region 2, the residual life-time of field-aged FKM O-rings, was 56.3 years based on the failure condition of $F_t/F_0 = 0.2$. By analyzing the degradation behavior and correlasting between equilibrium compression set and sealing force, we can predict the residual life-time of field-aged FKM O-rings.

Conclusions

Intermittent CSR jig was designed by considering how FKM O-rings are assembled. We could measure the seling force of a FKM O-ring by intermittent CSR testing, and sealing force of a FKM O-ring was 1.28 kN at room temperature. According to the number of intermittent CSR test, average sealing force of FKM O-rings was 1.27 kN, and deviation was ±4.5%. We observed the degradation behavior of O-rings with various thermal aging temperatures. With elevating aging temperature, degradation rate was increased. At 60°C, FKM O-rings didn't age sufficiently. Even after over 5,208 hrs, F_t/F_0 was only 0.914. By using TTS principle, we obtained stress relaxation master curve at 60°C. The time which FKM O-rings took to reach $F_t/F_0 = 0.2$, was respectively 48,760 hrs. We could save about 43,552 hrs of testing time by using TTS principle. From the relationship between α_T and 1000/T, we could calculate the activation energy, and observe the change of activation

energy according to thermal aging temperature range. At 100°C~170°C range, the activation energy was 64.5 kJ/mol. At 60°C~100°C range, the activation energy was 54.7 kJ/mol. By extrapolation, we calculated α_T as 0.088 at room temperature, and could draw the stress relaxation master curve at room temperature. As failure condition was selected as F_t/F_0 = 0.2, the life-time of FKM O-rings predicted as 66.2 years at room temperature. We measured compression set of aged FKM O-rings by testing the thickness of O-rings. Because of physical relaxation induced recovery of O-ring thickness, compression set of O-rings was decreased with time at room temperature. After 420 days, change of the compression set was 15.7% and compression set was still changing. By thermal treatment, physical relaxation could be accelerated and could be arrived to equilibrium state with short time. In here, thermal treatment which was two days at 80 °C, was recommended. Compression set which FKM O-rings were thermally treated two days, is 67.6%, and this was similar with 4,384 days maintained without thermal treatment. During 218 days, compression set which O-rings were thermally treated two days, changed just 0.5%. It seemed that O-rings almost arrived to equilibrium state. For observing the effect of chain scission and crosslinking reaction, we measured stress relaxation both strained and unstrained state. While F_t/F_0 was decayed with time-dependence, M_t/M_0 was increased. Because of M_t/M_0 (unstrained state) was affected both chain scission and crosslinking reaction. Average value of parameter *a* was 1.47, deviation was ±0.05. Parameter *a* showed uniform value distribution at whole aging processes. Because of it was greater than unity, we could confirm that crosslinking was relatively dominate chemical reaction of FKM O-rings at whole aging processes. For correlating between F_t/F_0 and equilibrium compression set, we measured equilibrium compression set of aged FKM O-rings. With empirical data of F_t/F_0 and equilibrium compression set, we could experimentally correlate the relationship between sealing force and equilibrium compression set. We confirmed that there was non-linear relationship between F_t/F_0 and equilibrium compression set. For predicting the residual life-time, we took out ten FKM O-rings which were 12.3 years field-aged in a propulsion unit. We measured equilibrium compression set of field-aged FKM O-rings according to the equilibrium compression set measurement procedures. Equilibrium compression set of field-aged FKM O-rings was 13.45%, and deviation was ±4.6%. By analyzing the relationship between sealing force and equilibrium compression set, F_t/F_0 of field-aged FKM O-rings was calculated to 0.909. We could convert the compression set to residual sealing force. By using stress relaxation master curve at 23 °C, we could predict the residual life-time of field-aged FKM O-rings as 56.3 years. By analyzing the degradation behavior and correlating between F_t/F_0 and equilibrium compression set, we could predict the residual life-time of 12.3 years field-aged FKM O-rings.

Author Contributions

Conceptualization, H.M.K. and M.C.C.; software, J.K.J., J.S.J., J.H.L., and N.K.C.; validation, H.M.K., M.C.C., J.K.J, and S.K.J.; formal analysis, M.C.C.; investigation, H.M.K., M.C.C.; writing-review and editing, Y.W.C. and J.H.L.; visualization, H.M.K., and M.C.C.; supervision, J.W.B.; project administration, J.W.B..

All authors have read and agreed to the published version of the manuscript.

Acknowledgments

This research was supported by The Development of Part using Fluorosilicone Material (20011150) project, The Development of -70°C Cryogenic, Hydrogen-resistant Elastomer for 70 MPa Hydrogen Tanks in Commercial Vehicles (RS-2024-00439388) project and The Development of High Vibration Damping Elastomers with Superior Durability (20011366) project, all supported by the Ministry of Trade, Industry and Energy.

Conflict of Interest: The authors declare that there is no conflict of interest.

References

1. R. P. Brown, Practical Guide to the Assessment of the Useful Life of Rubbers. RAPRA Technology Limited, UK.
2. R. P. Brown, and F. N. B. Bennett, “Compression stress relaxation”, *Polymer Testing,* **2**, 125 (2001).
3. S. Nishimura, “Fracture Behaviour of Ethylene Propylene Rubber for Hydrogen Gas Sealing under High Pressure Hydrogen”, *International Polymer Science and Technology,* **85**, 360 (2013).
4. Y. Zheng, Y. Tan, C. Zhou, G. Chen, J. Li, Y. Liu, B. Liao, and G. Zhang, “A review on effect of hydrogen on rubber seals used in the high-pressure hydrogen infrastructure”,

International Journal of Hydrogen Energy, **45**, 23721 (2020).
5. R. R. Barth, K. L. Simmons, and C. W. San Marchi, "Polymers for hydrogen infrastructure and vehicle fuel systems: applications, properties, and gap analysis. No.SAND2013-8904; 477341 (2013).
6. H. Ono, H. Fujiwara, and S. Nishimura, "Penetrated hydrogen content and volume inflation in unfilled NBR exposed to high-pressure hydrogen-What are the characteristics of unfilled-NBR dominating them?", *International Journal of Hydrogen Energy,* **43**, 18392 (2018).
7. A. Koga, T. Yamabe, H. Sato, K. Uchida, J. Nakayama, J. Yamabe, and S. Nishimura, "A Visualizing Study of Blister Initiation Behavior by Gas Decompression", *Tribology Online,* **8**, (2013).
8. J. Promchim, S. Kanking, P. Niltui, E. Wimolmala, and N. Sombatsompop, "Swelling and mechanical properties of (acrylonitrile-butadiene rubber)/(hydrogenated acrylonitrile-butadiene rubber) blends with precipitated silica filled in gasohol fuels", *Vinyl & Additive Technology,* **22**(3), 239 (2016).
9. J. K. Jung, I. G. Kim, K. S. Chung, Y. I. Kim, and D. H. Kim, "Determination of permeation properties of hydrogen gas in sealing rubbers using thermal desorption analysis gas chromatography", *Scientific Reports,* **11**, 17092 (2021).
10. M. C. Choi, J. H. Lee, Y. M. Yoon, S. K. Jeon, and J. W. Bae, "Long Term Reliability of Fluroelastomer (FKM) O-ring after Exposure to High Pressure Hydrogen Gas", *Elastomers and Composites,* **55**, 270 (2020).
11. J. Yambe and S. Nishimura, "Tensile Properties and Swelling Behavior of Sealing Rubber Materials Exposed to High-Pressure Hydrogen Gas", *Journal of Solid Mechanics and Materials Engineering,* **6**, 466 (2012).
12. H. Fujiwara, H. Ono, and S. Nishimura, "Degradation behavior of acrylonitrile butadiene rubber after cyclic high-pressure hydrogen exposure", *International Journal of Hydrogen Energy,* **40**, 2025 (2015).
13. H. Fujiwara, J. Yamabe, and S. Nishimura, "Evaluation of the change in chemical structure of acrylonitrile butadiene rubber after high-pressure hydrogen exposure", *International Journal of Hydrogen Energy,* **37**, 8729 (2012).
14. L. Ibarra, P. Posadas, and M. Esteban-Matrinez, "A comparative study of the effect of some paraffinic oils on rheological and dynamic properties and behavior at low temperature in EPDM rubber compounds", *Journal of Applied Polymer Science,* **97**, 1825 (2005).
15. S. W. Rutherford, R. E. Kurtz, M. G. Smith, K. G. Honnell, and J. E. Coons, "Measurement and correlation of sorption and transport properties of ethylene-propylene-diene monomer (EPDM) elastomers", *Journal of Membrane Science,* **263**, 57 (2005).
16. H. Ono, A. Nait-Ali, O. K. Diallo, G. Benoit, and S. Castagnet, "Influence of pressure cycling on damage evolution in an unfilled EPDM exposed to high-pressure hydrogen", *International Journal of Fracture,* **210**, 137 (2018).
17. J. Yamabe and S. Nishimura, "Nanoscale fracture analysis by atomic force microscopy of EPDM rubber due to high-pressure hydrogen decompression", *Journal of Materials Science,* **46**, 2300 (2011).
18. J. Yamabe, J. Matsumoto, and S. Nishimura, "Application of acoustic emission method to detection of internal fracture of sealing rubber material by high-pressure hydrogen decompression", *Polymer Testing,* **30**, 76 (2011).
19. J. Yamabe and S. Nishimura, "Influence of fillers on hydrogen penetration properties and blister fracture of rubber composites for O-ring exposed to high-pressure hydrogen gas", *International Journal of Hydrogen Energy,* **34**, 1977 (2009).
20. J. Yamabe and S. Nishimura, "Crack Growth Behavior of Sealing Rubber under Static Strain in High-Pressure Hydrogen Gas", *Journal of Solid Mechanics and Materials Engineering,* **5**, 690 (2011).
21. S. H. Lim, S. D. Lee, N. R. Lee, B. K. Ahn, N. Park, and W. H. Kim, "Effect of 1,3-Diphenyl-guanidine (DPG) Mixing Step on the Properties of SSBR-silica Compounds", *Elastomer and Composites,* **51**, 81 (2016).
22. P. J. Flory and J. Rehner, "Statistical Mechanics of CrossLinked Polymer Networks I. Rubber like Elasticity", *Journal of Chemistry and Physics,* **11**, 521 (1943).
23. Z. Hrniak-Murgic, J. Jelencic, >. Brayar, and M. Marovic, "Influence of the network on the interaction parameter in system EPDM vulcanizate-solvent", *Journal of Applied Polymer Science,* **65**, 991 (1997).
24. J. K. Jung, I. G. Kim, K. T. Kim, K. S. Ryu, and K. S. Chung, "Evaluation techniques of hydrogen permeation in sealing rubber materials", *Polymer Testing,* **93**, 107016 (2021).
25. J. K. Jung, I. G. Kim, S. K. Jeon, K. T. Kim, U. B. Baek, and S. H. Nahm, "Volumetric analysis technique for analyzing the transport properties of hydrogen gas in cylindrical-shaped rubbery polymers", *Polymer Testing,* **99**, 107147 (2021).
26. S. S. Choi, B. H. Park, and H. J. Song, "Influence of filler type and content on properties of styrene-butadiene rubber (SBR) compound reinforced with carbon black or silica", *Polymer Advanced Technologies,* **15**, 122 (2004).
27. H. Ismail, S. Ishak, and Z. Hamid, "Comparison Effect of

Mica and Talc as Filler in EPDM Composites on Curing, Tensile and Thermal Properties", *Progress in Rubber Plastics and Recycling Technology,* **29**, 109 (2013).
28. P. K. Pal and S. K. De, "Studies on peroxide vulcanization of silica-filled EPDM rubber in presence of vinyl silane coupling agent", *Polymer,* **25**, 855 (1984).
29. A. Mostafa, A. Abouel-Kasem, M. R. Bayoumi, and M. G. El-Sebaie, "Effect of carbon black loading on the swelling and compression set behavior of SBR and NBR rubber compounds", *Materials & Design,* **30**, 1561 (2009).
30. W. Arayapranee and G. L. Rempel, "A Comparative Study of the Cure Characteristics, Processability, Mechanical Properties, Ageing, and Morphology of Rice Husk Ash, Silica and Carbon Black Filled 75:25 NR/EPDM blends", *Journal of Applied Polymer Science,* **109**, 932 (2008).
31. M. S. Sohn, K. S. Kim, S. H. Hong, and J. K. Kim, "Dynamic mechanical properties of particle-reinforced EPDM composites", *Journal of Applied Polymer Science,* **87**, 1595 (2003).
32. N. Mandlekar, M. Joshi, and B. S. Butola, "A review on specialty elastomers based potential inflatable structures and applications", *Advanced Industrial and Engineering Polymer Research,* **5**, 33 (2021).
33. J. K. Jung, S. K. Jeon, U. B. Baek, and S. H. Nahm, "Development of Measurement Technology for Uptake and Diffusivity of Hydrogen Gas in Rubbers by Electronic Balances", *Journal of Hydrogen and New Energy,* **32**, 116 (2021).
34. K. L. Simmons, W. Kuang, S. D. Burton, B. W. Arey, Y. Shin, N. C. Menon, and D. B. Smith, "H-Mat hydrogen compatibility of polymers and elastomers", *International Journal of Hydrogen Energy,* **46**, 12300 (2021).
35. J. Yamabe and S. Nishimura, "Influence of carbon black on decompression failure and hydrogen permeation properties of filled ethylene-propylene-diene-methylene rubbers exposed to high-pressure hydrogen gas", *Journal of Applied Polymer Science,* **122**, 3172 (2011).
36. N. C. Menon, A. M. Kruizenga, A. Nissen, B. E. Mills, and J. Campbell, "Polymer Behaviour in High Pressure Hydrogen Gelium and Argon Environments as Applicable to the Hydrogen Infrastructure", Sandia National Lab. (SNL-NM), Albuquerque, NM (United States) (2017).